



Article

LiDAR-Derived Relief Typology of Loess Patches (East Poland)

Leszek Gawrysiak and Waldemar Kociuba *

Institute of Earth and Environmental Sciences, Maria Curie-Skłodowska University in Lublin,
20-031 Lublin, Poland; leszek.gawrysiak@mail.umcs.pl

* Correspondence: waldemar.kociuba@mail.umcs.pl; Tel.: +48-81-537-6853

Abstract: The application of the automated analysis of remote sensing data processed into high-resolution digital terrain models (DTMs) using geographic information systems (GIS) tools provides a geomorphometric characterization of the diversity of the relief of loess patches over large areas. Herein, a quantitative classification of 79 loess patches with a total area of 3361 km², distributed within the eastern part of the Polish Uplands belt, is carried out. A high-resolution 1 × 1 m DTM was generated from airborne laser scanning (ALS) data with densities ranging from 4 pts/m² to 12 pts/m², which was resampled to a resolution of 5 × 5 m for the study. This model was used to classify landform surfaces using the r.geomorphon (geomorphon algorithm) function in GRASS GIS software. By comparing the values in the neighborhood of each cell, a map of geomorphometric features (geomorphon) was obtained. The classification and typology of the relief of the studied loess patches was performed using GeoPAT2 (Geospatial Pattern Analysis Toolbox) software. Pattern signatures with a resolution of 100 × 100 m were extracted from the source data grid, and the similarity of geomorphological maps within the signatures was calculated and saved as a signature file and segment map using the spatial coincidence method. The distance matrix between each pair of segments was calculated, and the heterogeneity and isolation of the maps were generated. R system was used to classify the segments, which generated a dendrogram and a heat map based on the distance matrix. This made it possible to distinguish three main types and eight subtypes of relief. The morphometric approach used will contribute to a better understanding of the spatial variation in the relief of loess patches.

Keywords: high-resolution DTM; geomorphons; GeoPAT2; relief segmentation and clustering; relief similarity; loess relief types



Citation: Gawrysiak, L.; Kociuba, W. LiDAR-Derived Relief Typology of Loess Patches (East Poland). *Remote Sens.* **2023**, *15*, 1875. <https://doi.org/10.3390/rs15071875>

Academic Editor: Pinliang Dong

Received: 3 February 2023

Revised: 20 March 2023

Accepted: 29 March 2023

Published: 31 March 2023



Copyright: © 2023 by the authors. Licensee MDPI, Basel, Switzerland. This article is an open access article distributed under the terms and conditions of the Creative Commons Attribution (CC BY) license (<https://creativecommons.org/licenses/by/4.0/>).

1. Introduction

Photogrammetric remote sensing technics, which have been developed for almost a century, provide valuable insights into quantifying land use, vegetation cover, urbanization or landform differences [1]. Since the 1960s, aerial photogrammetry has been supported by satellite imagery. The use of multispectral satellite imagery expanded the resource of available information to include mineralogical and geomorphological features [2]. Since the 1970s, the next step was the availability of Light Detection and Ranging (LiDAR) data [3]. In this technology, laser beams are used to measure the distance between the sensor and the surface of the object being measured. When the object of measurement is the ground, LiDAR data can be used to create high-resolution digital terrain models (DTMs) [4]. These types of data open up entirely new research opportunities in the field of quantitative relief analysis, including the attempt to classify relief, based on geomorphometric features derived from DTMs.

Remote sensing data, such as aerial and satellite imagery and LiDAR, which are supported by delimitation algorithms, are an effective tool for studying the structure and spatial differentiation of relief [5], including the pattern of loess patches [6–8]. Based on remote sensing, a detailed DTM simplifies the understanding of the relationship between the landform locations within loess patches and their geomorphological features, as well as

their delimitation. Xiong et al. [9] applied a landform-oriented flow-routing algorithm to the study of loess landform morphology by separating landforms into positive landforms (P)—represented by plateaus and ridges—and negative landforms (N)—represented by erosional forms, i.e., valleys and gullies. Aerial and satellite imagery, including the most recent imagery acquired via sensors mounted on unmanned aerial vehicles (UAV-mounted cameras), provides a detailed, high-resolution picture of the landscape [10]. These images have been used to study the typology of loess relief by identifying and mapping the difference in the main landform types, such as loess plateaus, ridges, valleys and gullies, as well as to study the regional distribution and spatial pattern of these landforms that occur within loess patches [11]. Unlike photogrammetric aerial and satellite imagery, in which the representation of the ground surface is a grid, LiDAR data is provided in the form of a point cloud irregularly covering the surface. This allows for much more efficient modeling of the ground surface [12,13], and therefore much more precise identification and mapping of the landforms occurring within loess patches, such as loess plateaus and ridges, valleys and gullies [14,15]. This also allows for the study of the spatial patterns of these landforms within loess patches on both regional and local scales [16].

Previous analyses of loess relief, which used DTMs and algorithms implemented in GIS software, were carried out on examples from China. Their results provided a different perspective on loess relief, thus encouraging such studies for loess relief in Poland. Studies on the geomorphological diversity of loess patches in the east of Poland were carried out by several authors basing on field mapping and analog studies of topographic maps. Most of these studies were focused on the occurrence and density of gullies, e.g., [17–20] the arrangement of closed depressions [21–26]. Maruszczak [27,28], Kęsik [29] and Buraczyński [30] described the typology of a “loess relief” landforms dataset. Maruszczak developed overview maps of the relief of loess patches in the east of Poland, distinguishing three groups of relief datasets that characterized plateaus, slopes and valley bottoms [28] and classifying loess patches into three categories linked to local relief [31].

The aforementioned research was based on the use of analog methods or a simple analysis in GIS, the results of which show the main relief element of loess areas in overview maps or morphometric maps illustrating the density and distribution of selected relief forms within the basic fields. Quantitative studies on relief with the use of geomorphons were carried out for the whole of Poland [5], and chosen parts representing different types of relief in Poland or the world, e.g., [32–35]. Dekavalla and Argialas [36] proposed a novel method of land surface classification with the use of geomorphons. Gawrysiak and Kociuba [37] used geomorphons to analyze changes in the morphology of a proglacial valley. Recently, Dyba and Jasiewicz [38] developed land surface types of Poland based on nine morphometric parameters.

2. Materials and Methods

2.1. Study Area

The study area comprises 11,400 km² and is located in the eastern part of Poland, including Lublin, the Wołyń Uplands and the Roztocze macroregions. It is divided into 15 mesoregions (Figure 1). Relief is typical for Polish uplands, with absolute heights in the range of 115–392 m a.s.l. and a mean height of 228 m a.s.l. Each mesoregion has unique relief linked to local relief and geological conditions, especially tectonics and the rocks’ resistance to weathering [39]. Some of the mesoregions are covered with Pleistocene loess deposits, resulting in the appearance of a so-called “loess relief” landforms dataset [27]. It consists mainly of different types of valleys (mainly gullies), plateaus with closed depressions and slopes.

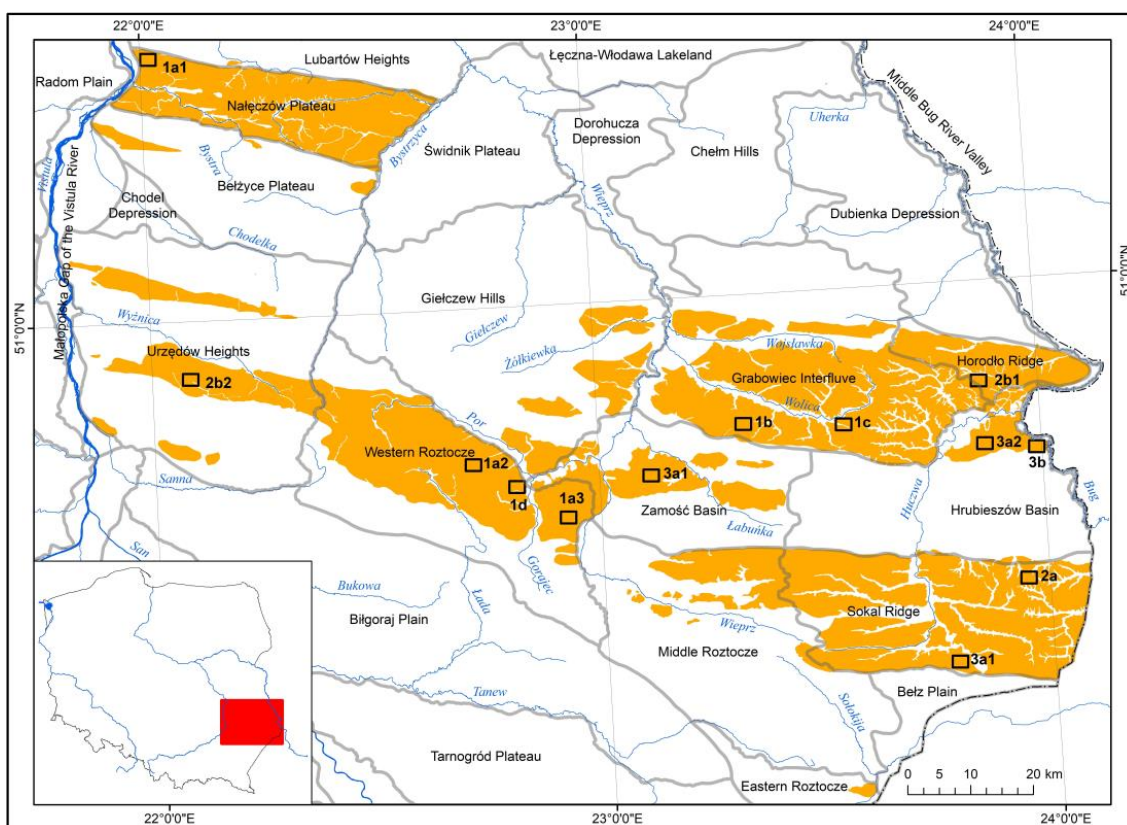


Figure 1. Localization of study area and extent of analyzed loess patches. Boundaries of physical-geographic regions (grey lines) and names, according to Solon et al. [40]. Small frames with numbers show the extent of sample geomorphon maps.

2.2. Mapping of Loess Patches

In this study, the relief of loess patches was analyzed. They form more than 70 isolated areas, covering 3361 km², and are arranged irregularly, usually in the W–E or WNW–ESE directions (Figure 1). Several maps of loess patches that extended over this area have been developed, e.g., by Maruszczak [28,31,41,42]. Other maps cover larger areas, usually Europe [8,43]. More detailed information on loess covers is included on geological and pedological maps, especially on the Detailed Geological Map of Poland 50 k, which is organized in sheets and shared on the website of the Polish National Geological Institute (<https://geologia.pgi.gov.pl/>, accessed on 1 January 2023).

Based on these developments, a new, detailed map of loess patches was created using GIS techniques. We also used a DTM and shaded relief map to accurately mark the boundaries of loess patches. Finally, 79 patches were marked (Figure 1) with a much better accuracy than previous developments.

2.3. DTM and Geomorphon Map

The digital terrain model (DTM) used in this elaboration is one of the products of the ISOK National Guard Information System project [44]. It is based on LiDAR scans of the whole of Poland with various densities, ranging from 4 pts/m² to 12 pts/m². Point clouds were processed into DEM layers (DTM, DSM and NDSM) with spatial resolutions of 1 × 1 m and were shared on the Geoportal website. DTMs files that covered the east of Poland were collected, merged and resampled to a resolution of 5 × 5 m. This resolution is optimal for these types of analyses [45]. It does not cause the quality of result maps to decline and significantly improves the speed of processing. To obtain hydrological correctness in the DTM, a fill tool (ArcGIS Pro) was used (Figure 2).

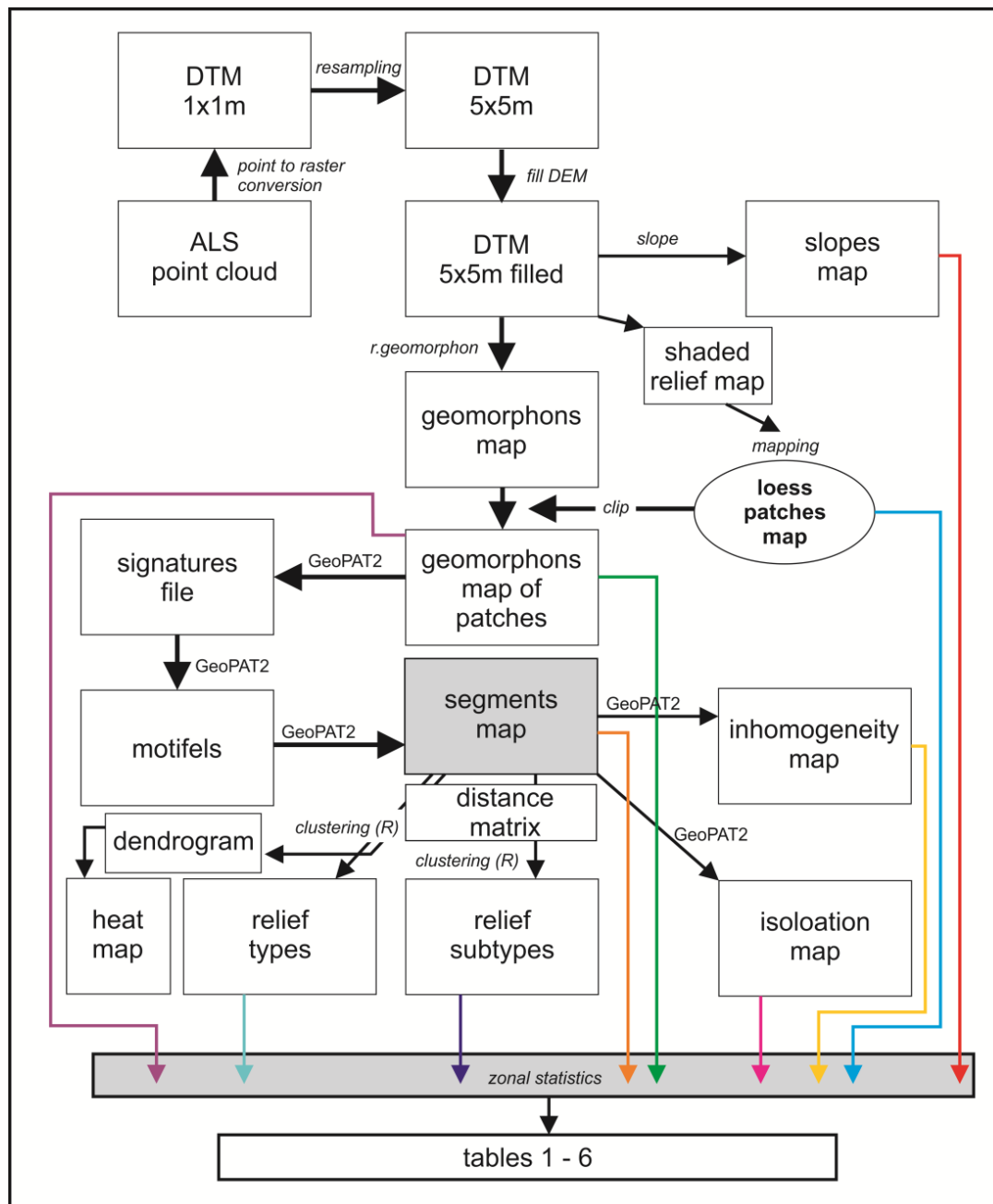


Figure 2. Flowchart of data processing and calculations.

The geomorphon map [5] was developed using the `r.geomorphon` function in GRASS GIS software. The geomorphon algorithm classified surface heights in DTM by comparing values in the neighborhood of each cell, using the inner (skip) and outer radius (search) and the flatness threshold (flat) as parameters. The result is a map of geomorphometric features consisting of ten elements: flat; peak; ridge; shoulder; spur; slope; hollow; footslope; valley; depression. Several scenarios of generating geomorphons were tested, including different values of the tool parameters. Finally, after visual verifications of the resulting maps, they were compared to standard geomorphological maps, and 10 m (skip), 100 m (search) and 1 (skip) values of these parameters were used.

2.4. Relief Analysis and Classification

Basic analyses of the relief of loess patches were realized using GeoPAT2 (Geospatial Pattern Analysis Toolbox) software [46], which is dedicated to large datasets using spatial

patterns. To study the relief of loess patches and to develop relief types and subtypes, a geomorphon map was used (Figure 2). The main algorithms implemented in GeoPAT2 are designed for extracting pattern signatures from a source data grid and additionally for geoprocessing and utilities. In the first step, signatures (100×100 m resolution) were made. The similarity of the geomorphon maps inside the signatures was then calculated, and it was recorded as the signatures file and grid file, using the spatial co-occurrence method [47]. This method is recommended for high-complexity patterns such as geomorphons [46]. Based on the signatures file, the distance matrix for each pair of segments was calculated using the Jensen–Shannon divergence [48]. The results of this analyses were polygon segments in which similar signatures were merged (Figure 3). To complete the analysis of the segments' inhomogeneity, isolation maps were generated using GeoPAT2. In order to classify the segments and combine them into types, hierarchical clustering [49] was performed using the R system and based on the distance matrix. The results were a dendrogram chart (Ward method) and a heat map. An analysis of the dendrogram, heat map and agglomeration curve distances (heights) was established to distinguish three main types and eight subtypes. Polygon shapefile maps, which contained segments grouped into types and subtypes of relief, were then generated. Finally, the statistical and spatial characteristics of the relief types and subtypes, summarized in tables, were created using the DTM, slopes, geomorphon maps and the distance matrix.

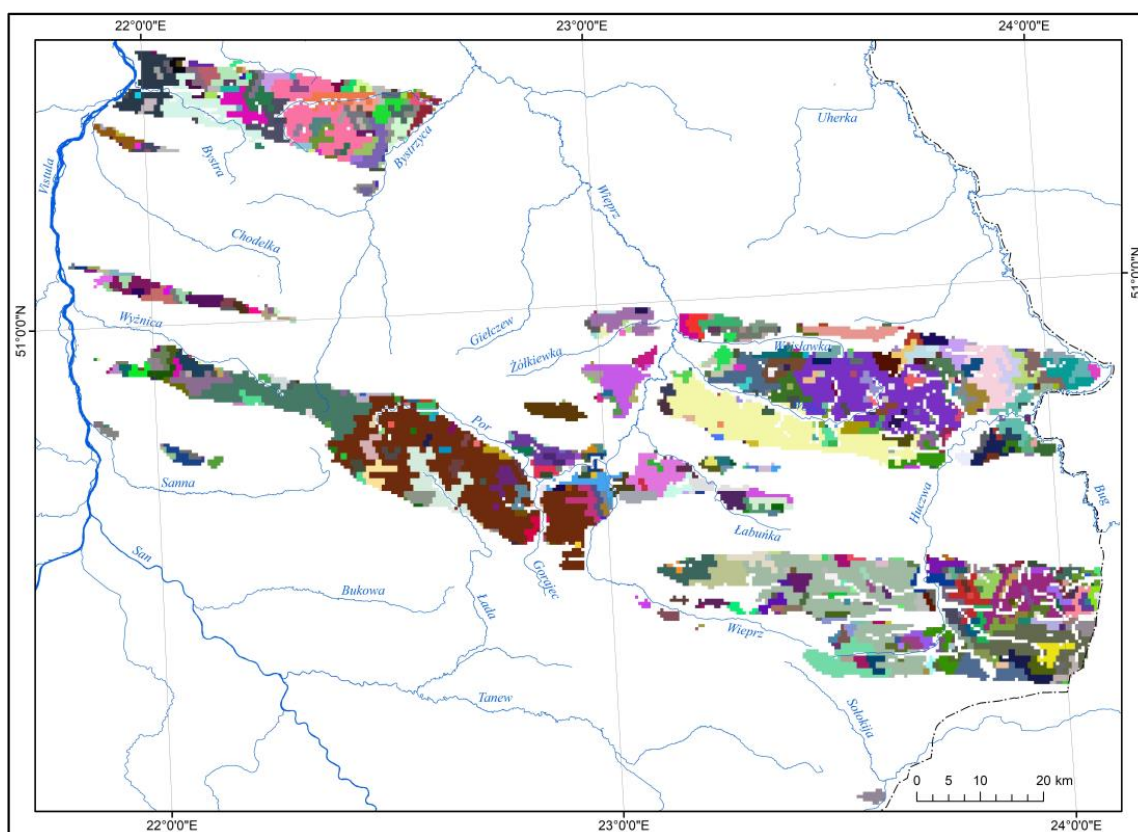


Figure 3. Unique relief segments of analyzed loess patches. Colors represent unique segments.

3. Results

3.1. Relief Types

The loess patches were divided into 647 segments (Figure 3, Table 1). The diversity of their relief was demonstrated. The area of the segments is strongly differentiated—the smallest segments are only 25 ha, while the largest reach 31,875 ha and cover the western side of Roztocze (Figure 1). The mean area is 525.58 ha. Subsequent segments, taking into account the area, are located on the Sokal Ridge and the Grabowiec Interfluve.

Table 1. Area characteristics (ha) of segments grouped into relief types and subtypes.

Type	Subtype	N *	Area (ha) **	Mean	Max	Min
High	Ha	79 (12)	67,625 (19.88)	856.0	31,875	25
	Hb	150 (23)	148,025 (43.54)	986.8	17,750	25
	Hc	71 (11)	10,650 (3.13)	150.0	925	25
	Hd	49 (8)	4525 (1.33)	92.3	475	25
	Whole type	349 (54)	230,825 (67.88)	661.4	31,875	25
Medium	Ma	80 (12)	27,275 (8.02)	340.9	6475	25
	Mb	128 (20)	49,350 (14.51)	385.5	4300	25
	Whole type	208 (32)	76,625 (22.53)	368.4	6475	25
Low	La	60 (9)	25,950 (7.63)	432.5	3450	25
	Lb	30 (5)	6650 (1.96)	221.7	675	25
	Whole type	90 (14)	32,600 (9.59)	362.2	3450	25
Total		647	340,050 (100)	525.6	31,875	25

* In brackets share of total number (%). ** In brackets share of total area (%).

This means that the relief within these patches is quite homogeneous over large areas. At the opposite end of the scale, there are highly differentiated [internally] lobes. The Nałęczów Plateau, previously considered quite homogeneous in terms of relief, is divided into a number of segments. Similarly, Horodło Ridge and the eastern part of Sokal Ridge are quite strongly differentiated internally.

The segments were classified into three classes which represent the main relief types of the loess patches. Type High (H) has the largest area and occupies 67.88% of the lobes. It usually creates very compact surfaces (Western and Middle Roztocze, Grabowiec Interfluve, Figure 4) or is mixed (spatially) with type Medium (M). This type is distinguished (Table 2) by the highest average height (246.9 m a.s.l.) and local relief (240.4 m). The average slope also has the highest value (5.53°). The share of geomorphons by type (Table 3) is also unique for this type of relief. The largest average height, the smallest flat surfaces and the largest ridge, spur, hollow, valley and depression prove that the carving in this type is intense, which justifies naming this type “High”. We decided to use this term to underline the intensity (dynamics) of the relief expressed by the high share of geomorphons located on the opposite sides of topography—plateaus and valleys. The subsequent groups are named based on this rule. Type Medium has a much smaller area (76,625 ha), constituting 22.53% of the patches. This type is not as compact as type H, and only on parts of Horodło and Sokal Ridges does it create distinct, larger surfaces. It also appears on the Nałęczów Plateau and in the western part of Urzędów Heights, but it is mixed with type H. The average height in this type is 224.5 m a.s.l., the local relief is 170.7 m and the average slope is less (2.49°) than in type H. Taking into account the share of geomorphon surfaces, this type also has unique features—all its values are between the High type and type Low; therefore, its proper name is the Medium type. The last type, Type Low(L), covers only 32,600 ha (9.59%) and contains only 90 segments. It occupies the largest areas in Zamość Basin, SE part of Giełczew Hills and several parts of Sokal, Horodło Ridge and Hrubieszów Basin. It is the lowest type—the average altitude is 214.9 m a.s.l., the local relief is 110.1 m and the average slope is 1.35°. This type is distinguished by the largest share of flat, shoulder and footslope geomorphons, and the slope occupies the smallest area here. Therefore, its name is “Low”.

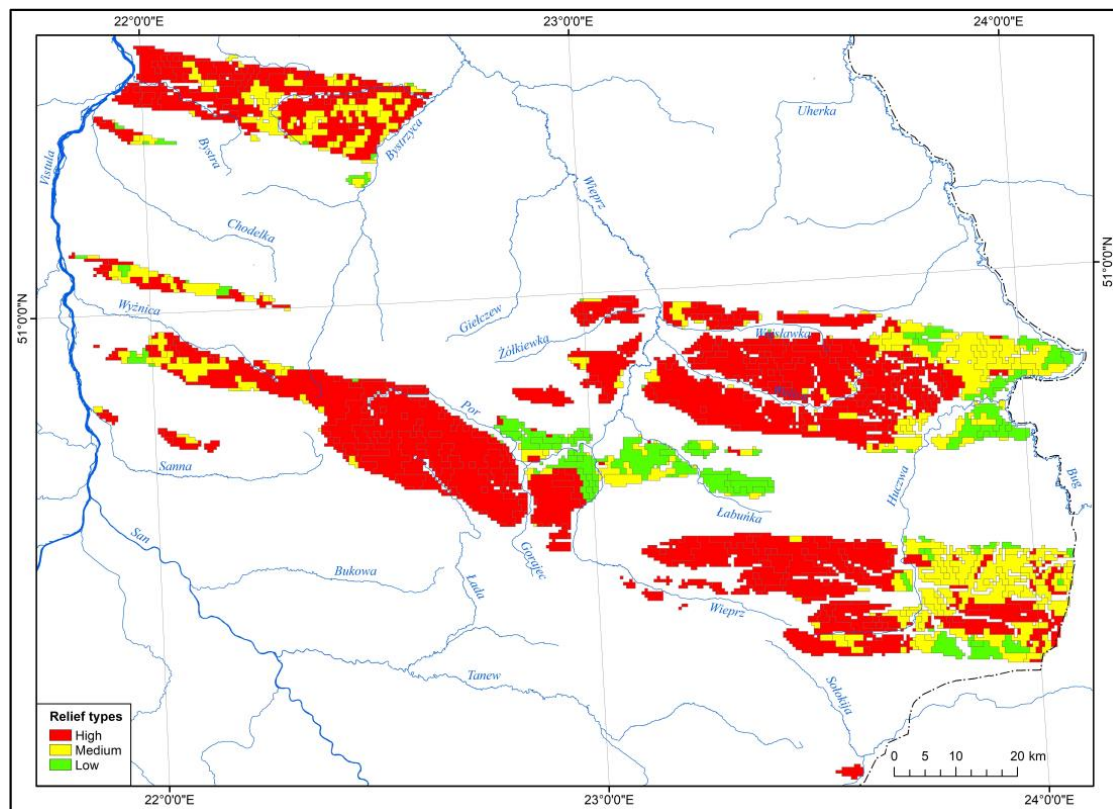


Figure 4. Segments of analyzed loess patches grouped in 3 main relief types.

Table 2. Basic morphometric characteristics of relief types and subtypes.

Type	Subtype	Mean Height (m a.s.l.)	Local Relief (m)	Mean Slope (°)
High	Ha	253.1	240.4	7.79
	Hb	245.1	218.0	4.62
	Hc	234.3	177.1	3.55
	Hd	247.1	188.7	6.17
	Whole type	246.9	240.4	5.53
Medium	Ma	228.4	138.5	2.72
	Mb	222.3	170.7	2.36
	Whole type	224.5	170.7	2.49
Low	La	216.4	110.1	1.44
	Lb	209.3	72.9	1.02
	Whole type	214.9	110.1	1.35
Total		238.8	240.4	4.45

Table 3. Share (%) of geomorphon types in area of relief types and subtypes.

Type	Subtype	Flat	Summit	Ridge	Shoulder	Spur	Slope	Hollow	Footslope	Valley	Depression
High	Ha	0.18	0.66	12.59	0.74	25.12	39.77	9.55	0.45	9.39	1.55
	Hb	0.89	0.52	8.95	2.30	19.33	45.65	10.51	1.53	9.91	0.41
	Hc	1.27	0.11	3.80	3.23	13.77	63.88	7.90	1.71	4.17	0.17
	Hd	0.03	0.21	6.82	0.32	19.81	56.62	8.19	0.34	7.24	0.42
	Whole type	0.68	0.54	9.77	1.84	20.82	44.89	10.07	1.20	9.46	0.74
Medium	Ma	5.04	0.17	5.13	8.04	12.00	49.85	8.39	5.02	6.30	0.07
	Mb	12.07	0.33	6.24	10.51	9.95	38.79	7.04	8.60	6.25	0.22
	Whole type	9.61	0.27	5.85	9.65	10.66	42.65	7.51	7.35	6.27	0.17

Table 3. Cont.

Type	Subtype	Flat	Summit	Ridge	Shoulder	Spur	Slope	Hollow	Footslope	Valley	Depression
Low	La	34.51	0.18	3.42	13.12	4.09	26.58	3.04	11.96	3.00	0.10
	Lb	61.93	0.08	1.65	10.18	1.63	12.90	1.16	9.18	1.24	0.04
	Whole type	40.16	0.16	3.05	12.52	3.59	23.76	2.65	11.39	2.64	0.09
Total		6.44	0.44	8.19	4.61	16.89	42.69	8.73	3.56	7.93	0.53

3.2. Relief Subtypes

The dendrogram chart (Figure 5A) and heat map (Figure 5B) reveal differentiation of the relief inside the three main types. The analysis of the agglomeration curve allowed for the indication of the boundary (dotted line in Figure 5A), which divides the set into eight subtypes that detail the image of the relief. Type “High”, has four subtypes, “Medium” has two subtypes and “Low” has two subtypes.

Within the “High” type, subtypes Ha and Hb clearly dominate, occupying 19.88% and 43.54% of the entire analyzed patch area, respectively (Table 1). Subtype Ha occurs in the western part of the Nałęczów Plateau and in the central part of Western Roztocze. Its small areas can still be found at the Grabowiec Interfluve and Middle Roztocze (Figure 6). This subtype has the highest values of mean height (253.1 m a.s.l.), local relief (240.4 m) and mean slope (7.79°). The surface share of particular types of geomorphons (Table 3) is the highest for summits, ridges, spurs, valleys and depressions, proving that this subtype has the most intense relief. The statistics of the distance matrix of this subtype (Table 4) and the structure of the dendrogram (Figure 5A) show that within this subtype, the relief has sub-subtypes with different degrees of internal similarity (distances in the matrix). This situation is repeated within all subtypes. Subtype Hb occupies the largest area on the Grabowiec Interfluve, the western part of Sokal Ridge, on the border of Urzędów Heights and Western Roztocze. This subtype is dominant on the Nałęczów Plateau, but its segments are mixed with subtype Mb. The average height (245.1 m a.s.l.) and the local relief (218 m) are lower than in subtype Ha. The mean values and standard deviation in the distance matrix (Table 4) are the lowest for this subtype, which proves that its segments are the least differentiated in terms of similarity. This subtype is distinguished by the largest share of hollow and valley areas in the entire “High” type (Table 3). Subtype Hc has a small area (3.13% of the total), and it usually occupies small segments located in the outer parts of loess patches. The lowest values of the average height, local relief and average slopes testify to the low intensity of its relief. This subtype has the largest proportion of the geomorphon slope. Its location on the dendrogram (Figure 5A) shows the lowest similarity to other subtypes within the “High” type. The last subtype, Hd (1.33% of the total area), is the most similar to subtype Hb (Figure 5A). It has a similar mean height and a lower local relief, but a higher mean slope. It occupies areas mainly within western Roztocze, Sokal Ridge and the Grabowiec Interfluve. A rather low mean value in the distance matrix and the lowest maximum value (Table 4) are evidence of the high similarity of segments within this subtype.

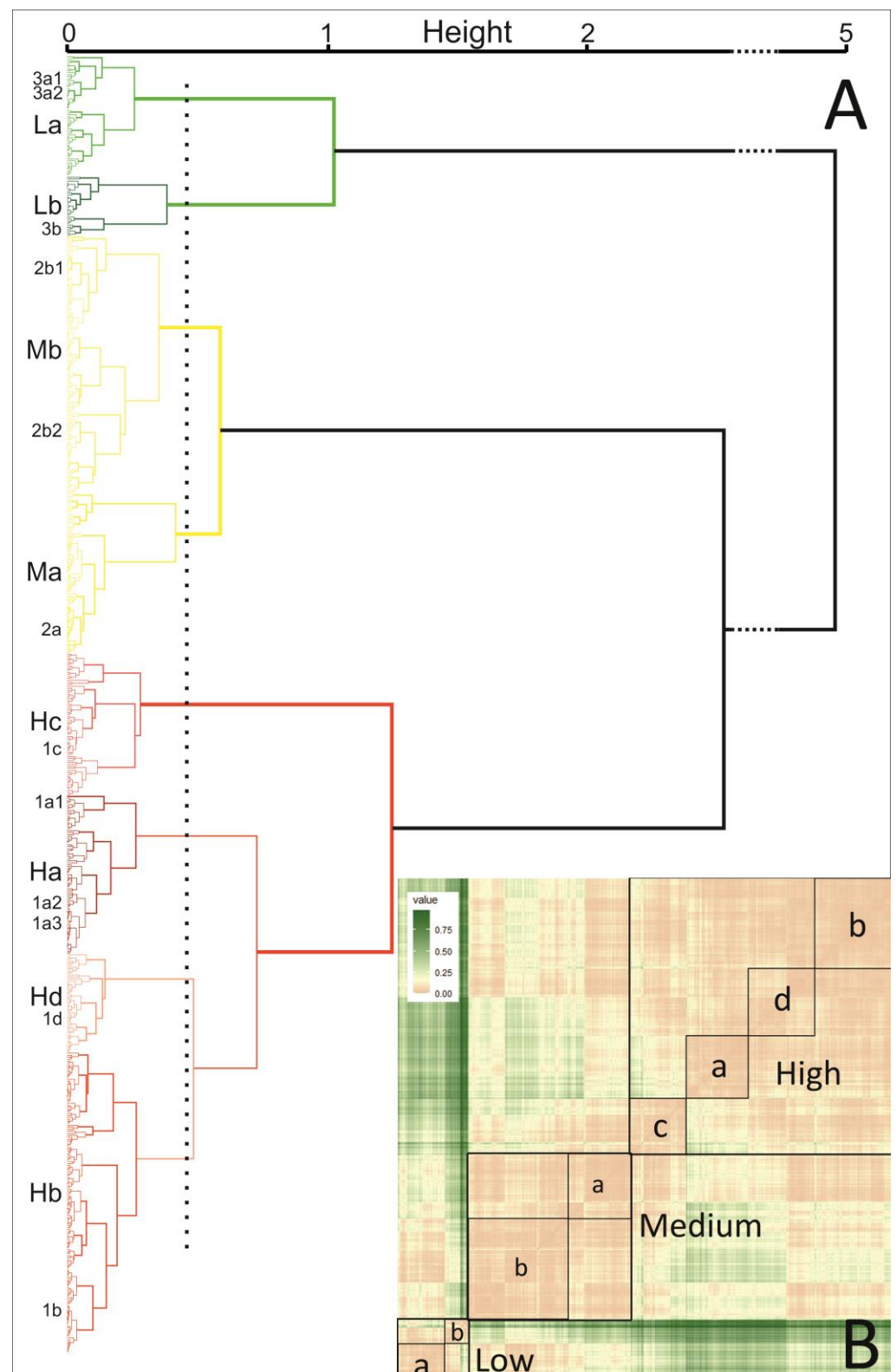


Figure 5. Dendrogram chart (A) and heat map (B) based on distance matrix between unique segments, grouped into relief types and subtypes. Dotted, vertical line marks the height of cutting, dividing the collection into 8 subgroups (subtypes). Small letters on vertical axis (1a1, 1a2, etc.) show location of the geomorphon example maps presented in Figure 6. Colors of types and subtypes on dendrogram are according to Figures 4 and 6.

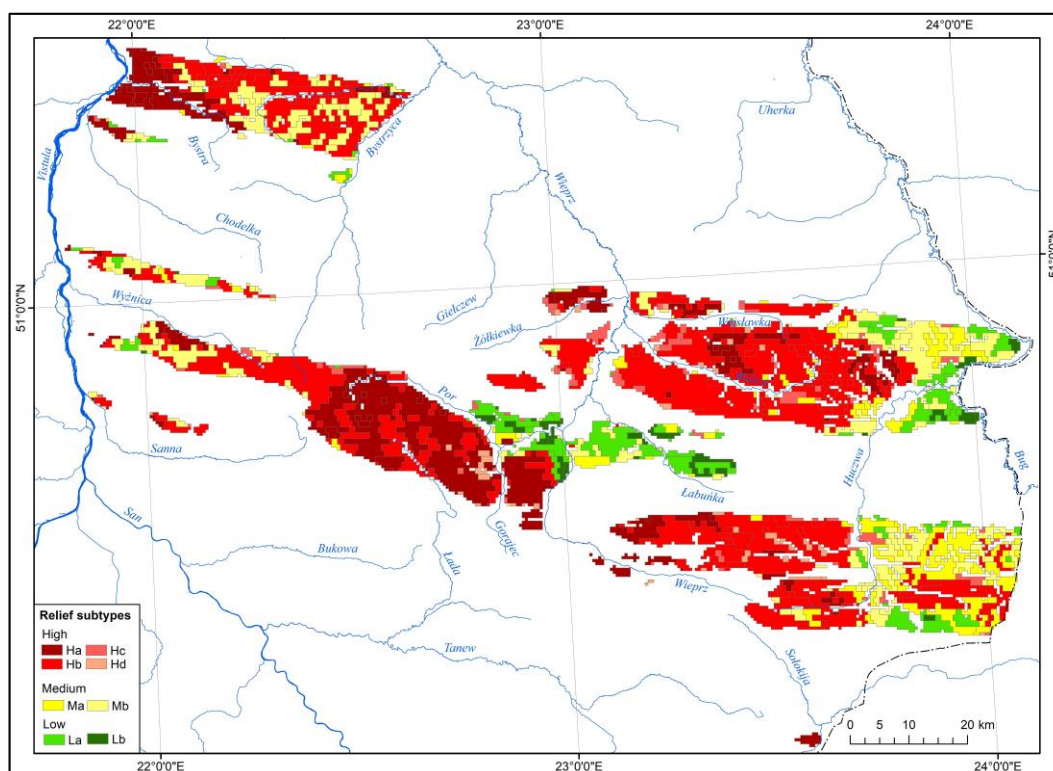


Figure 6. Subtypes of relief.

Table 4. Basic statistical parameters of segments' distance matrix, classified into relief types and subtypes.

Type	Subtype	Mean	Min	Max	Stdev
High	Ha	0.0390	0.0012	0.2596	0.0293
	Hb	0.0347	0.0006	0.1921	0.0215
	Hc	0.0526	0.0034	0.1803	0.0300
	Hd	0.0385	0.0036	0.1532	0.0217
	Whole type	0.0748	0.0006	0.6465	0.0748
Medium	Ma	0.0438	0.0010	0.2377	0.0355
	Mb	0.0438	0.0008	0.2730	0.0291
	Whole type	0.0564	0.0008	0.3332	0.0374
Low	La	0.0428	0.0015	0.1844	0.0286
	Lb	0.0639	0.0017	0.2700	0.0547
	Whole type	0.9006	0.0015	0.5257	0.0884
Total		0.1706	0.0006	0.9777	0.1632

Subtype Ma (8.02% of total area) mainly occupies the Horodło and the Sokal Ridges (Figure 6). It has a mean height (228.4 m a.s.l.) close to the mean of all patches, but a low local relief value (138.5 m). It is distinguished by the lowest share of the depression geomorphon and a high standard deviation of distance. Subtype Mb (14.51% of total area) usually co-occurs with Ma on the Horodło and Sokal Ridges, but it is also present on the Nałęczów Plateau and Urzędów Heights. It has a similar mean height to Ma (222.3 m a.s.l.), but a higher local relief (170.7 m), a similar mean slope and a clearly lower share of the slope geomorphon.

Subtype La (7.63% of total area) represents the relief of low located patches, mainly in the Hrubieszów and Zamość Basins as well as the same parts of the Horodło and Sokal Ridges (Figure 6). Its mean height (216.4 m a.s.l.) and local relief (110.1 m) are lower than the mean values for all the patches. It has a high share of the flat geomorphon

and highest (in all patches) share of the shoulder and footslope. Subtype Lb (1.96% of the total area) is the lowest, as evidenced by the values of its mean elevation (214.9 m a.s.l.), local relief (110.1 m) and mean slope (1.02°). It has the highest values of the mean distance and standard deviation among all subtypes, which proves that this subtype is internally the most diverse. Small segments of this subtype are located in the Zamość and Hrubieszów Basins.

Each subtype has its unique spatial pattern (Figure 7). Subtype Ha is highly differentiated internally and, consequently, it is easy to see clear differences. Example 1a1 shows the relief of the western part of Nałęczów Plateau (Figure 1), and examples 1a2 and 1a3 show the eastern part of Western Roztocze. Example 1a1 is located in the other part of the dendrogram then 1a2 and 1a3, which are located close to each other (Figure 5A). Examples 1b (Grabowiec Interfluve) and 1d (Western Roztocze) look different than what was previously describe above, but these subtypes are fairly close together. The most notable is 1c, whose ridges are not so visible. Examples 2a, 2b1 and 2b2 are quite similar, and some differences can be observed. Example 2a has more valleys, and 2b2 is distinguished from 2b1 by a larger share of flat areas. Example 3a1 represents the areas with the smallest share of flat areas; 3a2 has more of them, and 3b is the flattest.

3.3. Inhomogeneity and Isolation

Segments classified in terms of mutual dissimilarity demonstrate the inhomogeneity of the loess patches (Figure 8). Smaller values mean that the motifs of the segments are more similar to each other. Taking into account the inhomogeneity values of all patches, it can be concluded that the relief of the studied loess patches is fairly homogenous, the maximum value for which reaches only 0.1171, which is quite a low value (Table 5). However, regional differences can be observed. Low values (shades of green) forming large areas can be observed on the Nałęczów Plateau, Grabowiec Interfluve, western Roztocze and Sokal Ridge. The most notable is the dark green of the Nałęczów Plateau in which values in some segments have a value of 0, while in others the value is in the 0–0.015 range. Shades of yellow appear in the S part of the Nałęczów Plateau, on the border between Western Roztocze and Urzędów Heights, and in smaller areas on the Grabowiec Interfluve and the Sokal Ridge. The warmest colors (pink and red) usually form small areas on the smallest loess patches. In this regard, the Hrubieszów Basin also stands out.

In studying the values of the relief types and subtypes (Table 5), it can be found that the High type is the most differentiated, and the subtype Hb stands out from the rest. However, the mean value of the heterogeneity is the smallest. The “Low” type, in which the La subtype stands out, has the greatest value. The “Medium” type is located between the types described above.

Table 5. Changeability of values of inhomogeneity (IN) and isolation (IS) indices in relief types and subtypes.

Type	Subtype	IN-Mean	IN-Max	IS-Mean	IS-Max
High	Ha	0.0250	0.0533	0.0736	0.4589
	Hb	0.0316	0.1171	0.0791	0.3258
	Hc	0.0295	0.0799	0.1085	0.2814
	Hd	0.0089	0.0330	0.0514	0.1620
	Whole type	0.0291	0.1171	0.0783	0.4589
Medium	Ma	0.0365	0.0761	0.1140	0.3611
	Mb	0.0311	0.0969	0.1084	0.2981
	Whole type	0.0330	0.0969	0.1104	0.3611
Low	La	0.0394	0.0748	0.1523	0.3651
	Lb	0.0314	0.0750	0.1715	0.4182
	Whole type	0.0378	0.0750	0.1562	0.4182
Total		0.0308	0.1171	0.0931	0.4589

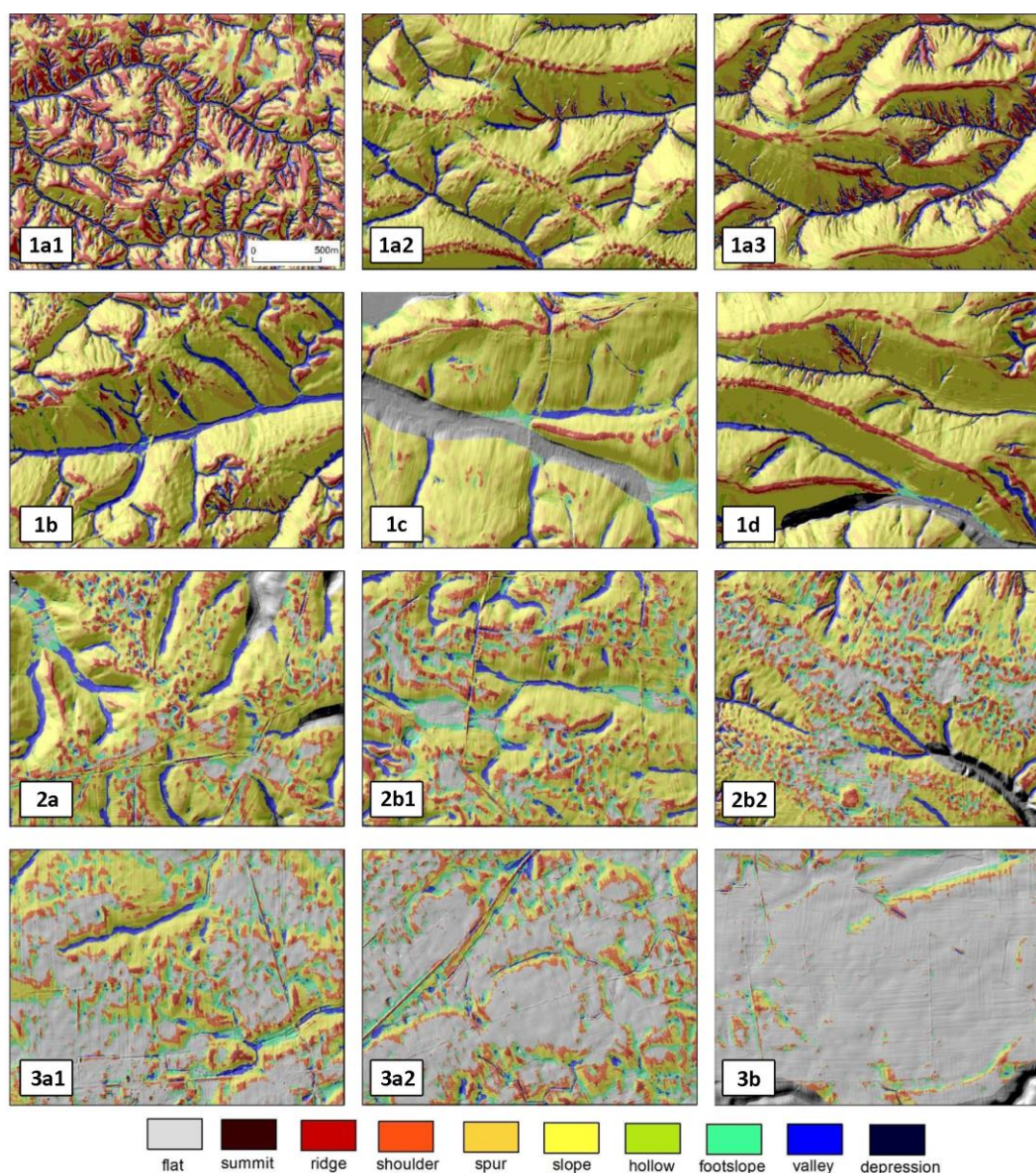


Figure 7. Example geomorphons maps of each relief subtypes. Localization of subfigures shown on Figure 1. Subfigures (1a1,1a2), (1a3) (Ha), (1b) (Hb), (1c) (Hc) and (1d) (Hd) represent subtypes of type “High”; (2a) (Ma), (2b1) and (2b2) (Mb) represent subtypes of type “Medium”; (3a1), (3a2) (La) and (3b) (Lb) represent subtypes of type “Low”.

The grade of isolation (Figure 9) shows an average dissimilarity between each segment and all of its immediate neighbors. Larger values (warm colors) indicate a higher isolation. The resulting map is dominated by cold colors, but local differences can be observed. Blue shadows occupy most of the area. Warmer colors occur in smaller patches on the border zones of other areas. The highest values (up to 0.4589) of isolation are reached in Urzędów Heights and in the Hrubieszów Basin. The High type has the lowest mean isolation value (Table 5), lower than the mean for all types, but the highest max value, proving a high internal, local anomaly. Subtype Hc stands out with the highest mean value. The Medium type has a moderate average value which is higher than the average value for all patches. The maximum values in the subtypes Ma and Mb are lower than the others in the dataset. The Low type has the highest mean value and high mean and maximum values among the subtypes.

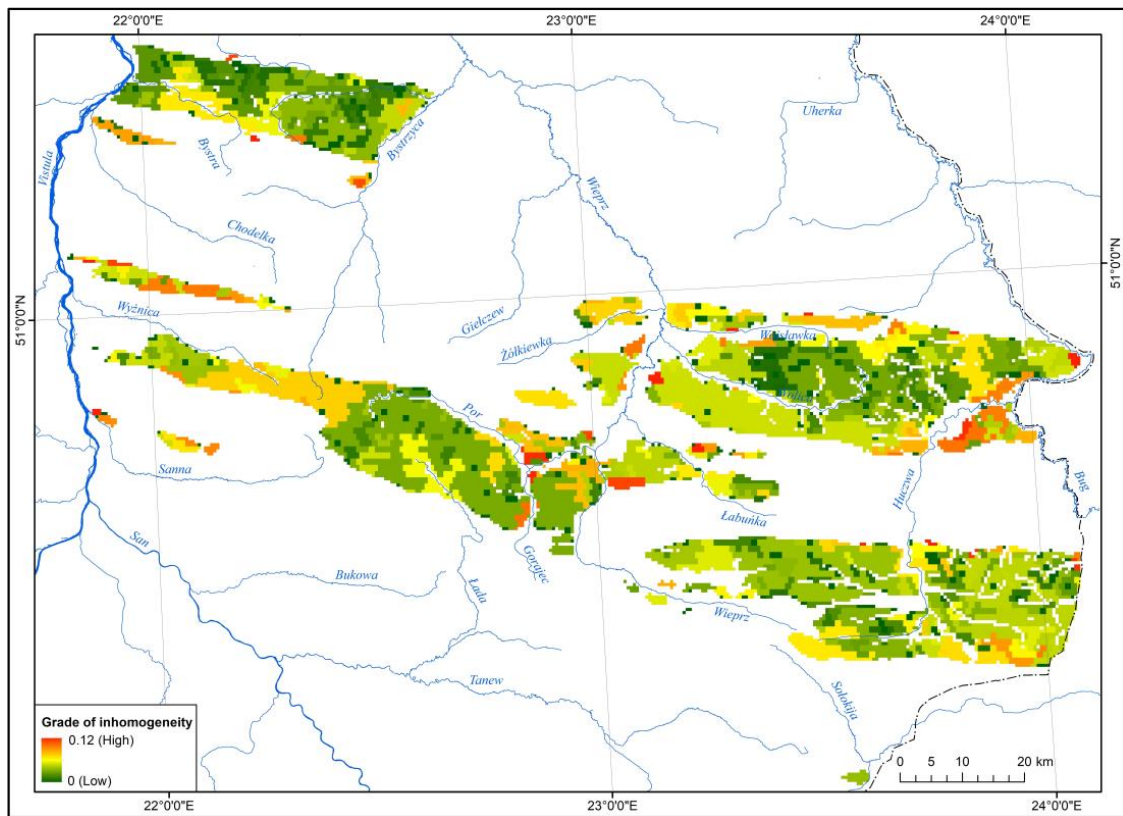


Figure 8. Grade of inhomogeneity of unique segments of loess patches.

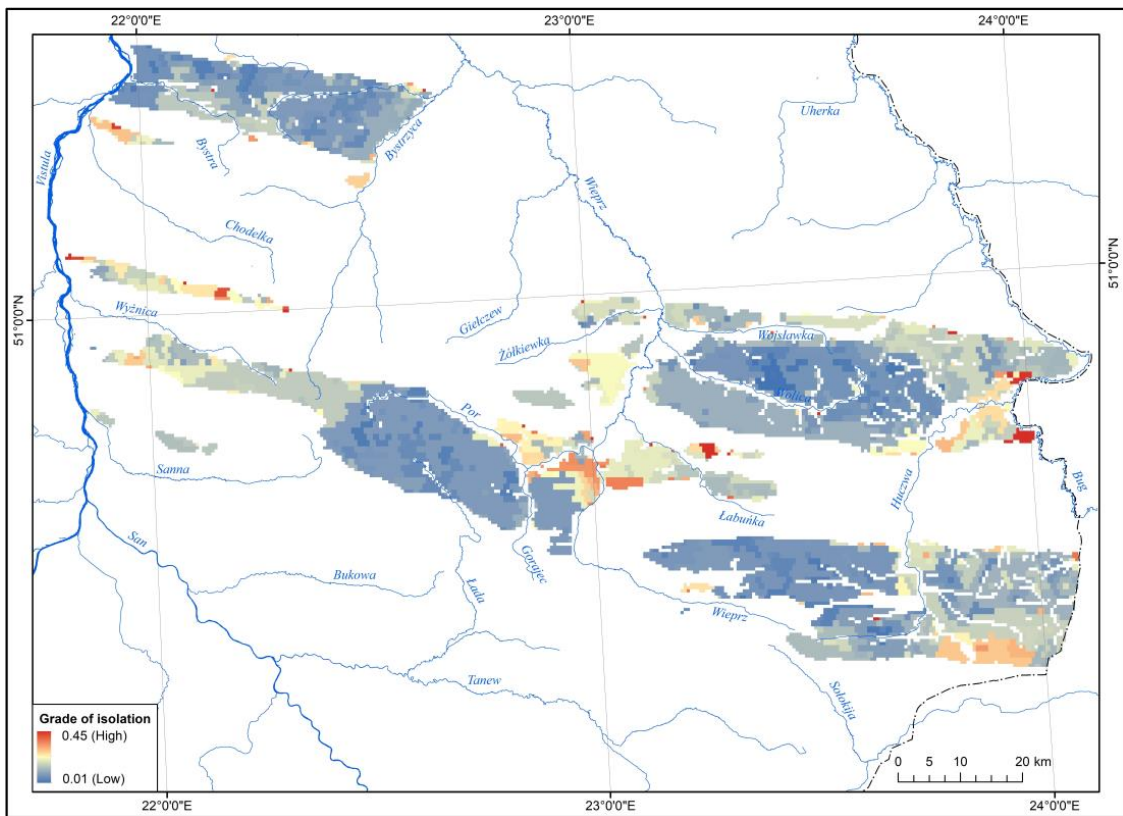


Figure 9. Grade of isolation of unique segments of loess patches.

4. Discussion

LiDAR-derived DTMs are changing the way geomorphologists study relief and its evolution, contributing to a more efficient conceptualization of landforms by studying their pattern and spatial variation. The classification of terrain morphology with geomorphons, proposed by Jasiewicz and Stepinski [5], enables the rapid and accurate description of morphological trends and patterns over large areas. This type of topographic texture analysis facilitates the understanding of the relationships between the distribution of geomorphometric features [50] and their morphometric characteristics [37]. LiDAR-derived DTMs are thus an optimal basis for the relief typology of loess landscapes [11,51]. At the same time, algorithms are becoming an increasingly popular tool for studying the diversity of loess patch relief [6–8,52]. However, a significant part of the research is concerned with the automatic delimitation of main relief elements in order to distinguish areas with a different direction of development and intensity of relief processes. Another important research problem is the proper selection of the resolution of DTMs, which determines the accuracy of the delimitation of individual landforms. Siłuch et al. [16] emphasized that both overly general (25–30 m) and very detailed (1 m) models can generate errors in automatic delimitation, resulting in the underestimation of morphometric features, respectively, or the generation of noise in the form of “non-existent” landforms that require additional verification. Therefore, the optimal solution in this situation seems to be the use of DTMs with a resolution of 5×5 m. High-precision DTMs with 5 m resolution have been successfully used to delimit the shorelines of eroded loess formations based on proper derivation method and the quantifying indexes system [53]. Flow steering algorithms, on the other hand, were used to separate intensively developing erosional forms (N) and stable top surfaces (ridge land and smooth surface) located above the shoulder-line (P) [9].

There are fewer studies focused on the typology of loess relief in which the goal is not only to identify and map the diversity of relief forms, such as loess ridges, plateaus, valleys and gullies. Therefore, the current study focuses on assessing the variations and possible regularities (spatial patterns) of the regional distribution of these forms within loess patches. Since loess and loess-like sediments cover as much as 10% of the Earth's surface [43], the effect of scale is important here. For this reason, the study covered the entire eastern part of the Polish Upland belt: an area of 11,295 km². Almost 80 patches, ranging from 0.04 km² to 614 km², were analysed. Their total area is 3361 km², that is, 29.8% of the common area of the eastern part of the Polish Uplands belt. A quantitative evaluation of relief was carried out using geomorphometric objects, identified using the geomorphon method [5], GeoPAT2 software [46] and algorithms of segmentation [54] and hierarchical clustering [49]. The applied multi-stage research process provided the basis to develop a typology of loess relief, taking into account its local and regional distinctive features. This approach, previously used for the entire area of Poland [5], was applied for the first time to a detailed analysis of loess relief differentiation.

The proposed framework allows for a detailed analysis of relief based on the similarity of designated motifs and segments, the end result of which is a relief classification distinguishing three types and eight subtypes. A quantitative estimation of the highlighted units in terms of a number of features/parameters (shares of geomorphic areas, absolute heights and local relief, slopes and similarity of segments) reveals their unique parameters and allows for the delimitation of areas with similar features. The analysis showed that the spatial patterns of relief occurring within the loess patches of the eastern part of the Polish Uplands belt relate to the leading parameters of the geomorphological regions in which they are located [39], and in particular to the density of the gully network [19,21] and local relief [21].

5. Conclusions

The studies were carried out for the upland part of eastern Poland, which is partly covered by loess deposits, forming loess patches that are clearly distinguishable in relief. The analysis covered an area of 3361 km², involving almost 80 isolated areas. It was shown

that quantitative studies on relief can be accomplished with the use of geomorphometric features (geomorphons) that are derived from LiDAR elevation data. Using dedicated software and algorithms, a typology of relief can be developed.

Detail analysis of relief, focused on the similarity of motifs and segments of loess patches, allowed the researchers to distinguish relief types and subtypes. It was noted that their spatial pattern correlated well with the main parameters of the studied upland area. Quantitative characteristics of types and subtypes, including the share of geomorphons, heights, slope and similarity of segments, revealed their unique parameters. The High type occupies the largest area (67.88%) and is distinguished by the highest mean elevation (246.9 m a.s.l.), with the local relief (240.3 m) and high mean slope (5.53°), and high areas' share of ridge (9.77%), spur (20.82%), hollow (10.07%), valley (9.46%) and depression (0.74%) geomorphons. This type has the largest mean area of segments (661.39 ha). The Low type has the lowest mean height (214.9 m a.s.l.), local relief (110.1 m) and mean slope (1.35°). Characteristic features of this type are the largest surfaces of flat, shoulder and footslope geomorphons and the smallest surface of slope. The Medium type is located "between" the High and Low types, and its morphometric characteristics are located in the middle (224.5 m a.s.l.; 170.7 m; 2.49°, respectively). The subtypes within the types have different characteristics, but the morphometric parameters and contributions [area] of the geomorphons clearly distinguish them from each other.

The result of the study is a typology of relief of loess patches, consisting of three types divided into eight subtypes. The main types, High, Medium and Low, and the subtypes have unique characteristics and internal structures, as documented by the presented maps, tables and charts. The spatial pattern of the relief typology shows clear regularities manifested in the localization, share of areas and the co-occurrence of the geomorphons' types.

Author Contributions: Conceptualization, L.G. and W.K.; methodology, L.G.; software, L.G.; validation, L.G.; formal analysis, L.G.; investigation, L.G.; resources, L.G. and W.K.; data curation, L.G. and W.K.; writing—original draft preparation, L.G. and W.K.; writing—review and editing, L.G. and W.K.; visualization, L.G.; supervision, W.K.; project administration, W.K.; funding acquisition, W.K. All authors have read and agreed to the published version of the manuscript.

Funding: This research received no external funding.

Data Availability Statement: The data presented in this study are available upon request from the corresponding author.

Acknowledgments: The authors would like to thank the Reviewers for their valuable comments that helped to make the improvements that were essential for the successful completion of this work. The authors are also grateful for the English language proofreading by Andrew Warchol.

Conflicts of Interest: The authors declare no conflict of interest.

References

1. Rees, W.G. *Physical Principles of Remote Sensing*, 3rd ed.; Cambridge University Press: Cambridge, UK, 2012; ISBN 978-1-107-00473-3.
2. Jensen, J.R. *Remote Sensing of the Environment: An Earth Resource Perspective*; Prentice Hall Series in Geographic Information Science; Prentice Hall: Upper Saddle River, NJ, USA, 2000; ISBN 978-0-13-489733-2.
3. Simpson, M.L.; Hutchinson, D.P. IMAGING | Lidar. In *Encyclopedia of Modern Optics*; Elsevier: Amsterdam, The Netherlands, 2005; pp. 169–178. ISBN 978-0-12-369395-2.
4. Bater, C.W.; Coops, N.C. Evaluating Error Associated with Lidar-Derived DEM Interpolation. *Comput. Geosci.* **2009**, *35*, 289–300. [[CrossRef](#)]
5. Jasiewicz, J.; Stepinski, T.F. Geomorphons—A Pattern Recognition Approach to Classification and Mapping of Landforms. *Geomorphology* **2013**, *182*, 147–156. [[CrossRef](#)]
6. Romanescu, G.; Lóczy, D.; Dezső, J.; Carboni, D. Loess-Scape in the Dobrudja Plateau (Romania). Landforms and Updated Typology. *Present Environ. Sustain. Dev.* **2018**, *12*, 95–114. [[CrossRef](#)]
7. Liu, K.; Ding, H.; Tang, G.; Song, C.; Liu, Y.; Jiang, L.; Zhao, B.; Gao, Y.; Ma, R. Large-Scale Mapping of Gully-Affected Areas: An Approach Integrating Google Earth Images and Terrain Skeleton Information. *Geomorphology* **2018**, *314*, 13–26. [[CrossRef](#)]
8. Lehmkühl, F.; Nett, J.J.; Pötter, S.; Schulte, P.; Sprafke, T.; Jary, Z.; Antoine, P.; Wacha, L.; Wolf, D.; Zerboni, A.; et al. Loess Landscapes of Europe—Mapping, Geomorphology, and Zonal Differentiation. *Earth-Sci. Rev.* **2021**, *215*, 103496. [[CrossRef](#)]

9. Xiong, L.; Tang, G.; Yan, S.; Zhu, S.; Sun, Y. Landform-Oriented Flow-Routing Algorithm for the Dual-Structure Loess Terrain Based on Digital Elevation Models: Flow-routing algorithms for the dual-structure loess terrain. *Hydrol. Process.* **2014**, *28*, 1756–1766. [[CrossRef](#)]
10. Jiménez-Jiménez, S.I.; Ojeda-Bustamante, W.; Marcial-Pablo, M.; Enciso, J. Digital Terrain Models Generated with Low-Cost UAV Photogrammetry: Methodology and Accuracy. *ISPRS Int. J. Geo-Inf.* **2021**, *10*, 285. [[CrossRef](#)]
11. Wei, H.; Li, S.; Li, C.; Zhao, F.; Xiong, L.; Tang, G. Quantification of Loess Landforms from Three-Dimensional Landscape Pattern Perspective by Using DEMs. *ISPRS Int. J. Geo-Inf.* **2021**, *10*, 693. [[CrossRef](#)]
12. Costantino, D.; Angelini, M.G. Production of DTM Quality by TLS Data. *Eur. J. Remote Sens.* **2013**, *46*, 80–103. [[CrossRef](#)]
13. Kociuba, W.; Kubisz, W.; Zagórski, P. Use of Terrestrial Laser Scanning (TLS) for Monitoring and Modelling of Geomorphic Processes and Phenomena at a Small and Medium Spatial Scale in Polar Environment (Scott River—Spitsbergen). *Geomorphology* **2014**, *212*, 84–96. [[CrossRef](#)]
14. Kociuba, W.; Janicki, G.; Rodzik, J. 3D Laser Scanning as a New Tool of Assessment of Erosion Rates in Forested Loess Gullies (Case Study: Kolonia Celejów, Lublin Upland). *Ann. UMCS Geogr. Geol. Mineral. Petrogr.* **2014**, *69*, 107–116. [[CrossRef](#)]
15. Kociuba, W.; Janicki, G.; Rodzik, J.; Stępniewski, K. Comparison of Volumetric and Remote Sensing Methods (TLS) for Assessing the Development of a Permanent Forested Loess Gully. *Nat. Hazards* **2015**, *79*, 139–158. [[CrossRef](#)]
16. Siłuch, M.; Kociuba, W.; Gawrysiak, L.; Bartmiński, P. Assessment and Quantitative Evaluation of Loess Area Geomorphodiversity Using Multiresolution DTMs (Roztocze Region, SE Poland). *Resources* **2023**, *12*, 7. [[CrossRef](#)]
17. Buraczynski, J. Erozja Wąwozowa Na Roztoczu—Międzyrzecze Gorajca i Wieprza. *Folia Soc. Sci. Lublinensis* **1975**, *17*, 2.
18. Buraczynski, J. Natężenie erozji wąwozowej i erozji gleb na roztoczu gorajskim. *Zesz. Probl. Postępów Nauk Rol.* **1977**, *193*, 91–99.
19. Maruszczak, H. Erozja Wąwozowa We Wschodniej Części Pasa Wyżyn Południowopolskich. *Zesz. Probl. Postępów Nauk Rol.* **1973**, *151*, 15–30.
20. Józefaciuk, C.; Józefaciuk, A. Gęstość Sieci Wąwozowej w Fizjograficznych Krainach Polski. *Pamiętnik Puławski* **1992**, *101*, 51–66.
21. Gawrysiak, L.; Harasimiuk, M. Spatial Diversity of Gully Density of the Lublin Upland and Roztocze Hills (SE Poland). *Ann. UMCS Geogr. Geol. Mineral. Petrogr.* **2012**, *67*, 27. [[CrossRef](#)]
22. Kołodyńska-Gawrysiak, R.; Chabudziński, Ł. Cechy Morfometryczne Oraz Rozmieszczenie Zagłębi Bezodpływowych Płaskowyżu Nałęczowskiego (Wyżyna Lubelska, E Polska). *Ann. UMCS Sect. B Geogr. Geol. Mineral. Petrogr.* **2014**, *69*, 45–61.
23. Kołodyńska-Gawrysiak, R.; Poesen, J. Closed Depressions in the European Loess Belt—Natural or Anthropogenic Origin? *Geomorphology* **2017**, *288*, 111–128. [[CrossRef](#)]
24. Kołodyńska-Gawrysiak, R.; Harasimiuk, M.; Chabudziński, Ł.; Jezierski, W. The Importance of Geological Conditions for the Formation of Past Thermokarst Closed Depressions in the Loess Areas of Eastern Poland. *Geol. Q.* **2018**, *62*, 685–704. [[CrossRef](#)]
25. Kołodyńska-Gawrysiak, R. Holocene Evolution of Closed Depressions and Its Relation to Landscape Dynamics in the Loess Areas of Poland. *Holocene* **2019**, *29*, 543–564. [[CrossRef](#)]
26. Maruszczak, H. Wertebry Obszarów Lessowych Wyżyny Lubelskiej. *Ann. UMCS Sect. B Geogr. Geol. Mineral. Petrogr.* **1954**, *8*, 123–268.
27. Maruszczak, H. Charakterystyczny Formy Rzeźby Obszarów Lessowych Wyżyny Lubelskiej. *Czas. Geogr.* **1958**, *29*, 335–354.
28. Maruszczak, H. Le relief des terrains de loess le Plateau de Lublin. *Ann. UMCS Sect. B Geogr. Geol. Mineral. Petrogr.* **1960**, *15*, 93–122.
29. Kęsik, A. Vallées Des Terrains Loessiques de La Partie Quest Du Plateau de Nałęczów. *Ann. UMCS Sect. B Geogr. Geol. Mineral. Petrogr.* **1960**, *15*, 123–155.
30. Buraczynski, J. Typy Dolin Roztocza Zachodniego. *Ann. UMCS Sect. B Geogr. Geol. Mineral. Petrogr.* **1968**, *23*, 47–86.
31. Maruszczak, H. Warunki Geologiczno-Geomorfologiczne Rozwoju Erozji Gleb w Południowej Części Województwa Lubelskiego. *Wiad. Inst. Melior. Użytk. Zielonych* **1963**, *3*, 19–44.
32. Dąbrowski, A.; Jasiewicz, J. Zastosowanie Form Morfometrycznych Do Analizy Zróżnicowania Wybranych Typów Powierzchni Na Obszarach Młodoglacjalnych. *Badania Fizjogr.* **2014**, *5*, 95–111.
33. Józsa, E.; Kalmár, P. Assessing the Applicability of EU-DEM Dataset to Landform Classification Using Geomorphons Approach: The Case Study of Eastern Mecsek Mountains Region. *Kartogr. List. Lett.* **2014**, *22*, 90–101.
34. Gawrysiak, L. *Segmentacje Rzeźby Terenu z Wykorzystaniem Metod Automatycznej Klasyfikacji i ich Relacja do Mapy Geomorfologicznej*; MCSU Press: Lublin, Poland, 2018.
35. Silveira, R.M.P.; Silveira, C.T. da Automated Hierarchical Classification of Landforms in the State of Paraná Supported by Digital Terrain Modeling. *Rev. Bras. Geogr. Física* **2015**, *8*, 1509–1523. [[CrossRef](#)]
36. Dekavalla, M.; Argialas, D. Evaluation of a Spatially Adaptive Approach for Land Surface Classification from Digital Elevation Models. *Int. J. Geogr. Inf. Sci.* **2017**, *31*, 1978–2000. [[CrossRef](#)]
37. Gawrysiak, L.; Kociuba, W. Application of Geomorphons for Analysing Changes in the Morphology of a Proglacial Valley (Case Study: The Scott River, SW Svalbard). *Geomorphology* **2020**, *371*, 107449. [[CrossRef](#)]
38. Dyba, K.; Jasiewicz, J. Toward Geomorphometry of Plains—Country-Level Unsupervised Classification of Low-Relief Areas (Poland). *Geomorphology* **2022**, *413*, 108373. [[CrossRef](#)]
39. Maruszczak, H. Wyżyny Lubelsko-Wołyńskie. In *Geomorfologia Polski*; PWN: Warszawa, Poland, 1972; pp. 340–384.

40. Solon, J.; Borzyszkowski, J.; Bidłasik, M.; Richling, A.; Badora, K.; Balon, J.; Teresa, B.-W.; Chab, L.; Dobrowolski, R.; Grzegorzczak, I.; et al. Physico-Geographical Mesoregions of Poland: Verification and Adjustment of Boundaries on the Basis of Contemporary Spatial Data. *Geogr. Pol.* **2018**, *91*, 143–170. [[CrossRef](#)]
41. Maruszczak, H. *Podstawowe Profile Lessów w Polsce*; MCSU Press: Lublin, Poland, 2001; Volume 2, ISBN 83-227-1723-7.
42. Maruszczak, H. *Podstawowe Profile Lessów w Polsce*; MCSU Press: Lublin, Poland, 1991; Volume 1.
43. Haase, D.; Fink, J.; Haase, G.; Ruske, R.; Pécsi, M.; Richter, H.; Altermann, M.; Jäger, K.-D. Loess in Europe—Its Spatial Distribution Based on a European Loess Map, Scale 1:2,500,000. *Quat. Sci. Rev.* **2007**, *26*, 1301–1312. [[CrossRef](#)]
44. Woźniak, P. High Resolution Elevation Data in Poland. In *Geomorphometry for Geosciences*; Adam Mickiewicz University: Poznań, Poland, 2015; pp. 13–14. ISBN 978-83-7986-059-3.
45. Tang, G.; Song, X.; Li, F.; Zhang, Y.; Xiong, L. Slope Spectrum Critical Area and Its Spatial Variation in the Loess Plateau of China. *J. Geogr. Sci.* **2015**, *25*, 1452–1466. [[CrossRef](#)]
46. Netzel, P.; Nowosad, J.; Jasiewicz, J.; Niesterowicz, J.; Stepinski, T. *Geopat 2: User'S Manual*; Cincinnati, OH, USA, 2018. [[CrossRef](#)]
47. Haralick, R.M.; Shanmugam, K.; Dinstein, I. Textural Features for Image Classification. *IEEE Trans. Syst. Man Cybern.* **1973**, *SMC-3*, 610–621. [[CrossRef](#)]
48. Lin, J. Divergence Measures Based on the Shannon Entropy. *IEEE Trans. Inform. Theory* **1991**, *37*, 145–151. [[CrossRef](#)]
49. Jasiewicz, J.; Netzel, P.; Stepinski, T.F. Landscape Similarity, Retrieval, and Machine Mapping of Physiographic Units. *Geomorphology* **2014**, *221*, 104–112. [[CrossRef](#)]
50. Wood, J.D. The Geomorphologic Characterization of Digital Elevation Models. Ph.D. Thesis, University of Leicester, Leicester, UK, 1996.
51. Wei, H.; Xiong, L.; Zhao, F.; Tang, G.; Lane, S.N. Large-Scale Spatial Variability in Loess Landforms and Their Evolution, Luohe River Basin, Chinese Loess Plateau. *Geomorphology* **2022**, *415*, 108407. [[CrossRef](#)]
52. Liu, K.; Na, J.; Fan, C.; Huang, Y.; Ding, H.; Wang, Z.; Tang, G.; Song, C. Large-Scale Detection of the Tableland Areas and Erosion-Vulnerable Hotspots on the Chinese Loess Plateau. *Remote Sens.* **2022**, *14*, 1946. [[CrossRef](#)]
53. Tang, G.; Xiao, C.; Jia, D.; Yang, X. *DEM Based Investigation of Loess Shoulder-Line*; Chen, J., Pu, Y., Eds.; Society of Photo-Optical Instrumentation Engineers: Nanjing, China, 2007; p. 67532E.
54. Niesterowicz, J.; Stepinski, T.F. Regionalization of Multi-Categorical Landscapes Using Machine Vision Methods. *Appl. Geogr.* **2013**, *45*, 250–258. [[CrossRef](#)]

Disclaimer/Publisher's Note: The statements, opinions and data contained in all publications are solely those of the individual author(s) and contributor(s) and not of MDPI and/or the editor(s). MDPI and/or the editor(s) disclaim responsibility for any injury to people or property resulting from any ideas, methods, instructions or products referred to in the content.